Mapping Land Cover and Estimating the Grassland Structure in a Priority Area of the Chihuahuan Desert

Alberto Rodríguez-Maturino [1], José Hugo Martínez-Guerrero [2] (ID), Isaías Chairez-Hernández [3], Martín Emilio Pereda-Solis [2], Federico Villarreal-Guerrero [4], Marusia Renteria-Villalobos [4] and Alfredo Pinedo-Alvarez [4],*

[1] Programa Institucional de Doctorado en Ciencias Agropecuarias y Forestales, Universidad Juárez del Estado de Durango, Durango 34307, Mexico; maturino_al@yahoo.com

[2] Facultad de Medicina Veterinaria y Zootecnia, Universidad Juárez del Estado de Durango, Durango 34305, Mexico; che_hugo1@hotmail.com (J.H.M.-G.); conplandg@hotmail.com (M.E.P.-S.)

[3] Instituto Politécnico Nacional, CIIDIR, Durango 34220, Mexico; ichairez@hotmail.com

[4] Facultad de Zootecnia y Ecología, Universidad Autónoma de Chihuahua, Chihuahua 31453, Mexico; fvillarreal@uach.mx (F.V.-G.); mrenteria@uach.mx (M.R.-V.)

* Correspondence: apinedo@uach.mx; Tel.: +52-614-434-0363 (ext. 15); Fax: +52-614-434-0345

Abstract: A field characterization of the grassland vegetation structure, represented by the coverage of grass canopy (CGC) and the grass height, was carried out during three years (2009–2011) in a priority area for the conservation of grasslands of North America. Landsat Thematic Mapper (TM5) images were selected and the information of reflectance was obtained based on the geographical location of each field-sampling site. Linear models, constructed with field and satellite data, with high coefficients of determination for CGC ($R^2 = 0.81$, $R^2 = 0.81$ and $R^2 = 0.72$) and grass height ($R^2 = 0.82$, $R^2 = 0.79$ and $R^2 = 0.73$) were obtained. The maps showed a good level of CGC (>25%) and grass height (>25 cm), except for the year 2009, which presented the lowest values of grass height in the area. According to the Kappa Index, a moderate concordance among the three CGC maps was presented (0.49–0.59). Conversely, weak and moderate concordances were found among the grass height maps (0.36–0.59). It was observed that areas with a high CGC do not necessarily correspond to areas with greater grass height values. Based on the data analyzed in this study, the grassland areas are highly dynamic, structurally heterogeneous and the spatial distribution of the variables does not show a definite pattern. From the information generated, it is possible to determine those areas that are the most important for monitoring to then establish effective strategies for the conservation of these grasslands and the protection of threatened migratory bird species.

Keywords: remote sensing; modelling; coverage; grass height; Cuchillas de la Zarca

1. Introduction

Given their great biodiversity and the environmental services they provide; grasslands are ecosystems of great importance. According to Adams et al. [1] grasslands account for 40.5% of the Earth's surface and therefore play an important role in the global carbon cycle [2]. Currently, these ecosystems are undergoing significant deterioration due to overgrazing, urbanization, land use change, the presence of invasive species and habitat fragmentation [3–5]. Indeed, Hoesktra et al. [6] considered that grasslands are the most threatened ecosystems on Earth. Consequently, many species of migratory birds that use grasslands as habitat in the North American deserts have declined their populations continuously and steadily [7,8]. Previous studies on grasslands have focused on herbaceous productivity trends and on the factors that may affect the herbaceous coverage [9,10]. For instance, from studies on grasslands of the Chihuahuan Desert, which is distributed in northern

Mexico and the southern United States of America, some studies have focused on listing the plant species, on studies of its fauna and on its ecosystem fragmentation [11,12]. However, more research is needed on the spatio-temporal variation of the coverage of grass canopy (CGC) and grass height. This topic is particularly relevant because these variables are strongly related to the habitat quality for migratory birds and because the grasslands immersed in the Chihuahuan Desert do not escape from the issues and pressures that characterize this ecosystem [13,14].

One of the tools widely employed for monitoring habitat quality is remote sensing. This tool offers the possibility of studying extensive areas with a wide temporal margin at a low cost [15,16]. Data from the thematic mapper (TM) sensor (Landsat 5 satellite) provides the capability to perform synoptic monitoring. The Landsat archive provides detailed and consistent data about the change dynamics experienced in the terrestrial ecosystems [17–20]. The spectral data provided by the sensor have allowed the determination of the structural characteristics and composition of plants in various ecosystems [21–23]. Some of the parameters that have been correlated to habitat quality are CGC and grass height, parameters that have been employed to estimate the net annual biomass productivity of grasslands in the field. However, these kinds of methodologies require a significant investment of time and economic resources [24]. Thus, the use of remote sensing tools represents an alternative for the determination of grassland variables in a more economical and faster manner [25].

Several studies have shown the condition of winter habitat as a determining factor in the decline of some grassland avian species. In fact, the abundance and distribution of the native species of the Chihuahuan Desert, such as *Ammodramus bairdii*, *A. savannarum*, *Anthus spragueii*, *Calcarius ornatus* and *Pooecetes gramineus,* are strongly related to the structure of the grasslands, as well as to variables such as CGC and grass height [14,26]. Therefore, it is very important to obtain information about the dynamics of the grassland where the structural variables are highly susceptible for drastic changes in relatively short periods [27]. The objective of this study was to determine the spatial and temporal variations of CGC and grass height during a period of three years in an area under conservation called Cuchillas de la Zarca, located within the Chihuahuan Desert in Mexico.

2. Materials and Methods

The area of Cuchillas de la Zarca (CUZA) is a priority region for the conservation of grasslands and is located within the Chihuahuan Desert. This desert grassland is the most extensive in North America and is recognized for having high species richness despite being a dry area. In CUZA we can find both transition areas dominated by grasslands and extensive plains covered by them [28]. The area of CUZA is located between the coordinates 105°04′30.86″ W and 24°41′41.28″ N, as well as 104°57′07.48″ W and 25°27′04.24″ N. It comprises the northern part of the state of Durango and the southern part of the state of Chihuahua, Mexico. It has an area of 11,600 km^2 (Figure 1). The vegetation consists mainly of induced pasture, natural grassland, microphyll desert scrub, chaparral areas and pine-oak forest. In each of these vegetation types, grass species of the genera *Bouteloa, Aristida, Buchloe, Andropogon, Melinis, Muhlenbergia, Sporobolus, Heteropogon* and *Pleuraphis* may be present [29,30].
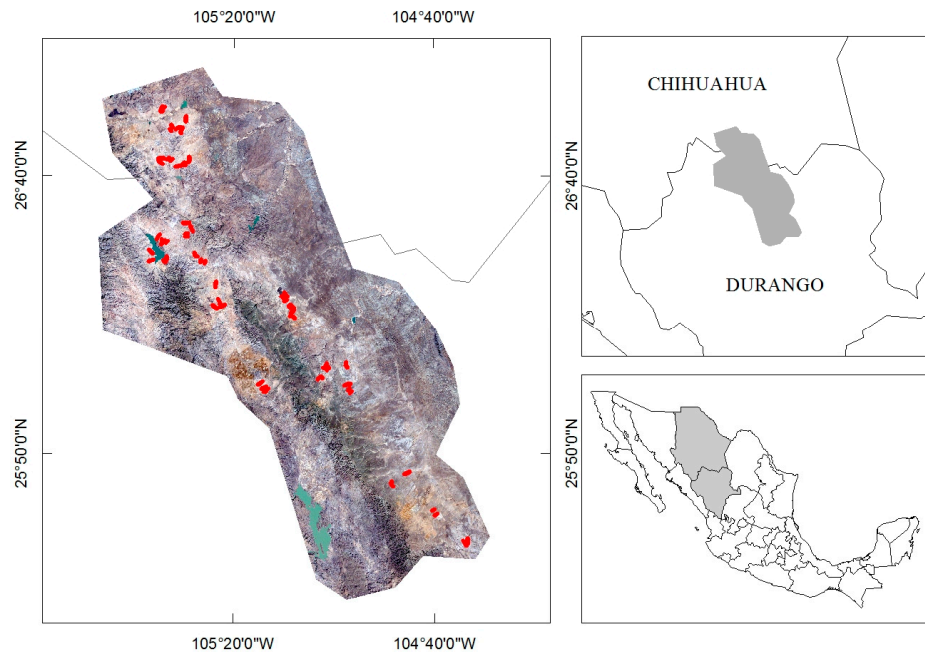
Figure 1. Study area. Sampling sites are marked in red.

2.1. Samples and Processing Date

The grassland structure, represented by CGC and grass height, was characterized during January and February by 96 transects in 2009, as well as 102 transects in 2010 and 2011. The transects of one kilometer of length were located according to a grid of squares with side lengths of 18 km covering the study area (Figure 2). The grid design was based on information from vector files of land use and roads network [31]. From all the 17 quadrants, only those with roads of acceptable condition were selected for easy access to the sampling points (red marks, Figure 1), which were located at every 500 m in each quadrant, as was established in a previous study [14]. For vegetation sampling, only the first three points of each quadrant were selected. In them, two sampling transects, perpendicular to the path, were established. Along the transects, circles of 5 m of radius were located each 100 m. In these circles, the area covered by grass canopy was visually assessed and the heights of three plants were measured at the ground level. For the height measurements, a small, a medium and a tall plant were chosen. From the three values, an average was estimated. All the measurements were made by only one person. For a summary of field data, the average CGC and grass height were obtained.
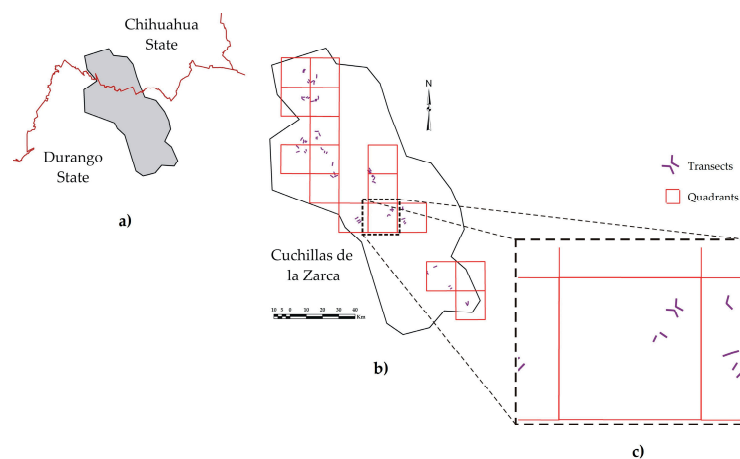
Figure 2. Spatial location of the samples within the study area.

Two scenes (path/row 31/41 and 31/42) of Landsat TM5 were acquired for each of the studied years from the United States Geological Survey (USGS) Global Visualization Viewer (GloVis, https://www.usgs.gov). The Landsat images correspond to the date of ground measurements, 5th February in 2009, 8th February in 2010, and 11th February 2011. For each year, the scenes were merged into a single mosaic.

To establish the relationship between the variables of vegetation structure and spectral values, the spectral information of the digital number (DN), extracted from the bands 1–5 and 7 of the sensor, the radiometrically-corrected values of reflectance and three synthetic bands, generated for the tasseled cap (TC), were correlated with CGC and grass height. The obtained bands of TC corresponded to the components of brightness (B), greenness (G) and wetness (W) [32]. The radiometric calibration was made by converting the gross value of each pixel (DN) into values of absolute spectral radiance. To reduce the variability among scenes, the spectral radiance was converted into exoatmospheric top of the atmosphere (TOA) reflectance. Formulae and coefficients provided by Chander et al. [33], represented by Equations (1) and (2), were used to perform the radiometric corrections applied to the TM sensor.

$$L_\lambda = \left(\frac{Lmax_\lambda - Lmin_\lambda}{QCALmax - QCALmin} \right) \times (QCAL - QCALmin) + Lmin_\lambda \tag{1}$$

$$\rho_\lambda = \frac{\pi \times L_\lambda \times d^2}{ESUN_\lambda \times \cos\ \theta_s} \tag{2}$$

where QCAL is DN; QCALmin and QCALmax are the minimum and maximum quantized calibrated pixel values, respectively; $Lmin_\lambda$ is the spectral radiance scales to QCALmin; $Lmax_\lambda$ is the spectral radiance scales to QCALmax; d is the distance from the earth to the sun; $ESUN_\lambda$ is the mean solar exoatmospheric irradiance; and θ_s is the solar zenith angle.

The atmospheric correction seeks to reduce or eliminate the image distortions resulting from the interaction of the atmosphere components with the sensor [34]. Such correction allows the standardization of image data and thus permits a comparison of images from different dates. From each of the circles of vegetation sampling located in the transects, the value of reflectance and TC components for each band were obtained from the corresponding pixel. Although some bushes and forests exist in the area, when sampling of vegetation in areas dominated by pasture, the sensor data were mainly associated to the spectral signatures of pastures. The bands that best explained the variables of CGC and grass height were selected to feed the models.

2.2. Statistical Analysis

The normality of the variables was proven with the Shapiro–Wilk test. After checking it, an analysis of variance was applied to determine if the differences among the quadrants were significant. Subsequently, multiple regression models [35] were run to explore the relationships of CGC and grass height with the spectral data. The CGC and grass height were established as response variables while the spectral data were used as independent variables. The spectral data included the DN, reflectance values and the values from the tasseled cap. The models were produced separately by dependent variable and by year. Once the models were obtained, the Gauss–Markov assumptions, which include normality, independence and homogeneity of variance, were verified on the data. To verify normality, the test was applied to the residuals of each model; to check independence, it was determined whether the correlation between the residual and predicted values were zero; and, to verify the homogeneity of variance, it was verified whether the correlation between the absolute value of the residuals and predicted values were close to zero ($p > 0.05$).

2.3. Maps of Cover of Grass Canopy and Grass Height

The estimators of the selected full models were used to construct maps of the variables CGC and grass height. For the case of CGC (%), their continuous values were reclassified in the following five classes: water bodies, 0–25 (low), 25–50 (medium), 50–75 (high) and 75–100 (very high). For the case

of grass height (cm), the classes were water bodies, 0–25 (low), 25–50 (medium), 50–75 (high) and >75 (very high). To make a comparison between the resulting maps, a cross-tabulation of images was made. Such a cross-tabulation determines the frequency of pixels that stayed constant during the evaluation period and serves to make inferences about the dynamics of CGC and grass height through time in the study area. Through this operation, the categories of a raster image were compared with those of a second image; both images had to have the same number of categories and the same data type. The operation casts the Kappa Index (KI) as a measure of agreement. The KI ranges from zero, indicating that there is no agreement, and up to one, indicating perfect agreement [36,37].

2.4. Meteorological Data

Given that information about precipitation in the study area was scarce, vector files from the National Meteorological Service, providing information on drought events occurring in the country, were used. These data are based on obtaining and interpreting indicators such as the standardized precipitation index (SPI), precipitation percent anomaly, satellite vegetation health index (VHI), NOAA/CPC leaky bucket soil moisture model, the normalized difference vegetation index (NDVI), the average temperature anomaly, the water availability percentage in the country's dams and the contribution of local experts. These indicators are displayed in the form of layers in a geographic information system and, by consensus, the drought-affected regions are determined according to a scale of intensities ranging from abnormally dry, moderate drought, severe drought, drought extreme and exceptional drought. As a result of the consensus, polygons for the intensity of drought were delineated, generating shape files. When the polygons correspond to the mid-month analysis (issued on the 15th day of each month) they are used to quantify the drought on the domestic territory. Likewise, when the polygons correspond to the final evaluation of the month, they complement the regional or continental map of the North American Drought Monitor [38]. Weather information linked to drought events was used to explain the different scenarios shown by the maps, considering that these events are related to precipitation and, in turn, rains occurring in a given year can largely explain the grassland conditions [39].

3. Results

3.1. Field Data

The average CGC ranged between 50%–75% and there were no differences between the three years ($p > 0.05$). Conversely, significant differences in grass height (cm) were found among the years studied ($p < 0.05$). The lowest values were recorded in 2009 (Table 1).

Table 1. Average (or mean) of field data for Coverage of Grass Canopy (CGC) and grass height in the quadrants measured in Cuchillas de la Zarca.
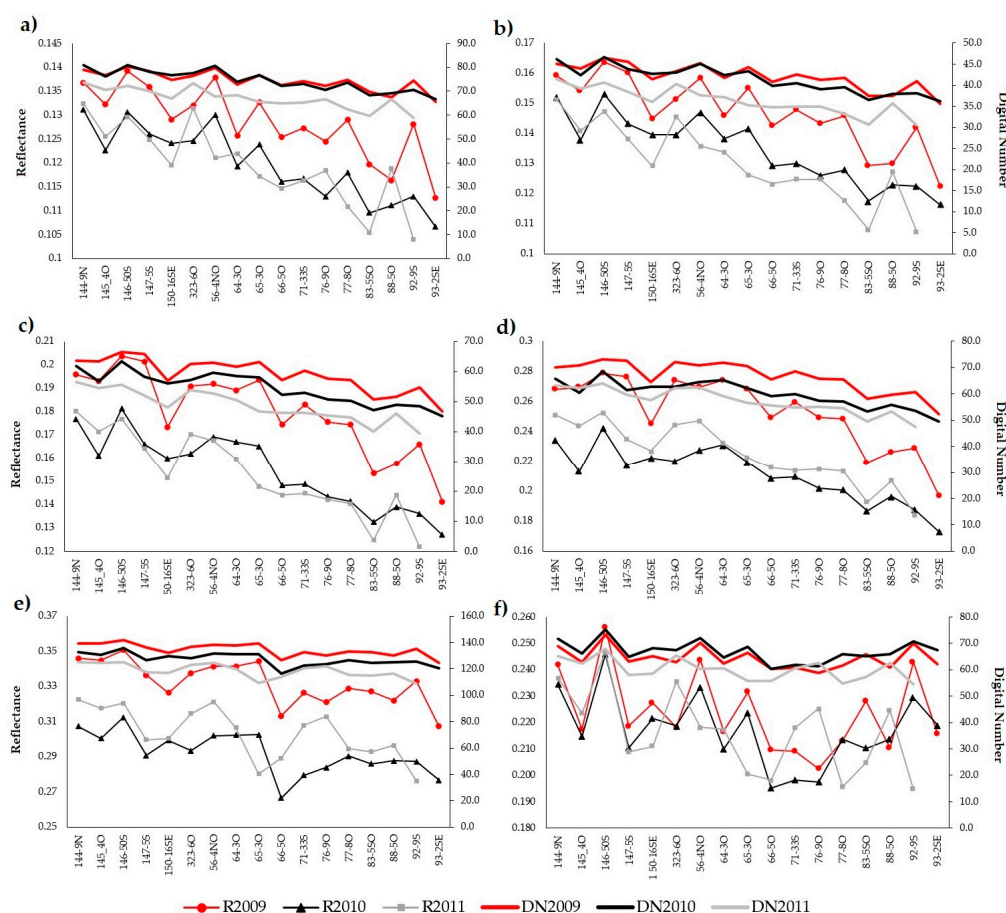
QUADRANT	CGC (%)			Grass Height (cm)		
	2009	**2010**	**2011**	**2009**	**2010**	**2011**
1	65.5	57.8	54.3	9.0	13.5	12.2
2	63.0	58.8	59.9	15.8	25.9	30.8
3	50.7	49.8	44.1	13.4	8.2	7.3
4	68.1	61.2	66.0	16.9	28.9	27.6
5	57.7	45.4	55.6	19.8	15.8	12.5
6	49.8	52.7	46.1	8.7	10.6	9.4
7	67.1	69.5	67.8	19.6	30.2	32.7
8	60.6	51.2	55.2	8.3	15.4	11.3
9	60.6	58.3	61.9	9.2	25.5	20.0
10	65.1	65.3	60.2	13.2	20.1	17.4
11	70.9	62.9	65.5	11.9	21.3	23.5
12	60.5	53.8	57.5	8.7	15.9	20.0

QUADRANT	CGC (%)			Grass Height (cm)		
	2009	**2010**	**2011**	**2009**	**2010**	**2011**
13	66.5	41.8	50.8	11.2	22.6	15.9
14	49.5	51.2	53.7	12.4	20.6	21.7
15	41.3	26.6	27.5	7.0	9.7	9.8
16	36.0	16.8	22.3	10.4	15.3	19.8
17	-	64.0	64.0	-	27.3	24.4

3.2. Spectral Data

The digital numbers and reflectance values followed the same pattern over the three years evaluated; bands 5, 7 (middle-infrared) and 4 (near-infrared) registered the highest values. A decline of reflectance was observed for the quadrants located in the central and southeast parts of the study area, particularly from the bands 1–3 (blue, green and red, respectively). In 2011, the values from the bands 2–4 and 7 showed a slight difference compared to the other two years (Figure 3).

Figure 3. Spectral signature average expressed as reflectance and the digital number for each quadrant ((**a**) band1, (**b**) band2, (**c**) band3; (**d**) band4, (**e**) band5, (**f**) band7).

Forty-two models for CGC and grass height were obtained. They corresponded to three years, two dependent variables, three elements of TC with the original bands, radiometrically-corrected bands and three transformations of dependent with independent variables. Six of the models were selected, one for each variable per year. The selected models met the Gauss–Markov assumptions, and had the lowest statistical deviance information criterion, Akaike information criterion, Bayesian information

criterion, (DIC, AIC, BIC) and the Root Mean Square Error (RMSE). In all the cases, the selected models only used images from bands into original digital values or in combination with an element of the TC. The coefficients of determination for the six models were high and with a significant probability ($p < 0.01$). In addition, the validation tests allowed us to verify the usefulness of each model, since the values of the mean square error of validation were slightly lower than those of calibration (Table 2).

Table 2. Coefficients of determination of linear regression models ($p < 0.01$).

Variable	Year	Statistics					Mean Square Error	
		R2	DIC	AIC	BIC	RMSE	Training	Validation
CGC	2011	0.81	11945	753.51	776.6	10.55	115.5	114.4
	2010	0.81	11945	753.51	776.59	11.15	118.7	117.4
	2009	0.72	10090	630.01	649.07	11.23	92.0	91.3
Grass Height	2011	0.82	0.38	−265.1	−244.1	0.060	50.2	48.7
	2010	0.79	0.49	−215.8	−192.7	0.071	69.5	68.7
	2009	0.73	6027.2	588.8	607.8	0.067	67.3	65.9

DIC = Deviance Information Criterion, AIC = Akaike Information Criterion, BIC = Bayesian Information Criterion, RMSE = Root Mean Square Error, CGC = Coverage of Grass Canopy.

For CGC, the best selected models for 2010 and 2011 used the bands in combination with the B element of the TC. For 2009, the model only used bands (Table 3). Similarly, the grass height models of 2009 and 2011 used only bands. Conversely, the models of 2010 used both the bands and the W element of TC (Table 4).

Table 3. Estimators of the regression models for coverage grass canopy (CGC).

Year	Intercept	B1	B2	B3	B4	B5	B7	TCb
2011	−8.5	2.2	−6.9 *	1.9	0.9	0.3	−2.3 *	0.7
2010	29	1.6	−1.8	3.0	2.0	2.3	−2.8 *	−2.4
2009	−5.4	2.5	−4.9	3.8	−1.9	1.7 *	−3.4 *	N/A

(B = band; 1,2,4,5,7 = band number; TCb = b element of the Tassaled Cap band; * $p < 0.01$).

Table 4. Estimators of the regression models for grass height.

Year	Intercept	B1	B2	B3	B4	B5	B7	TCw
2011	0.51 *	0.02	−0.07 *	0.04 *	−0.01	0.01 *	−0.02 *	
2010	0.87 *	0.03 *	−0.03	0.06 *	0.02	−0.06	−0.06 *	−0.09
2009	88.4 *	−2.04	4.1	0.12	−0.61	0.87 *	−2.6 *	

(B = band; 1,2,4,5,7 = band number; TCw = w element of the Tassaled Cap band; * $p < 0.01$).

3.3. Distribution Maps of CGC, Grass Height and Kappa Index

The selected models allowed the obtainment of CGC maps for three years (Figures 4a, 5a and 6a). According to the Kappa Index, among all the CGC maps a moderate concordance was presented, which was slightly higher between 2009 and 2010 and lower between 2010 and 2011 (Table 5). This was perhaps due to the fact that in 2009 and 2010 much of the surface of the study area presented a higher CGC (50–75%), while in 2011 the predominant interval was mainly located in low or intermediate levels (25–50%), as can be seen in Figure 4a. In 2009, the areas with higher CGC were in the zones of grassland and in the desert scrub. For 2010, the highest CGC was found in the northwest, a zone in which grassland areas and oak-pine forest are predominant. A similar pattern of distribution of the classes was seen in 2010 and 2011, although in a lower and more dispersed way for the latter.

As in the case of CGC, three maps of grass height were obtained from the selected models (Figures 4b, 5b and 6b). Based on the Kappa index only, a moderate concordance was presented between the maps of 2010 and 2011, while 2009 had a weak concordance for the two years (Table 5). According to the graph of the surface of the grass height ranges (Figure 7), the basic difference among the years with moderate concordance lay mainly in the fact that during 2009 the interval with the highest frequency was 0–25 cm, and for 2010 and 2011 it was 50–75 and 25–50 cm, respectively. Regarding 2009, it was characterized by grasses of low grass height along almost all of CUZA, only 8% of the area had a height of grass in the range of 25–50 cm, located primarily in the oak-pine areas. In 2010, the taller-height range (50–75 cm) was distributed generally almost along the entire area, except for the southeastern region, where grasslands with a lower grass height prevailed. Grasslands of greater grass height (>75) were conserved in both forest-oak and grassland areas. In 2011, the height ranges had a behavior similar to 2010, except that in the former, the range with the greatest presence was 25–50 cm in 57.2% of the area. In terms of distribution, the lowest grasses were in the oak-pine forests, whereas the middle and taller heights were distributed more or less uniformly through the area.
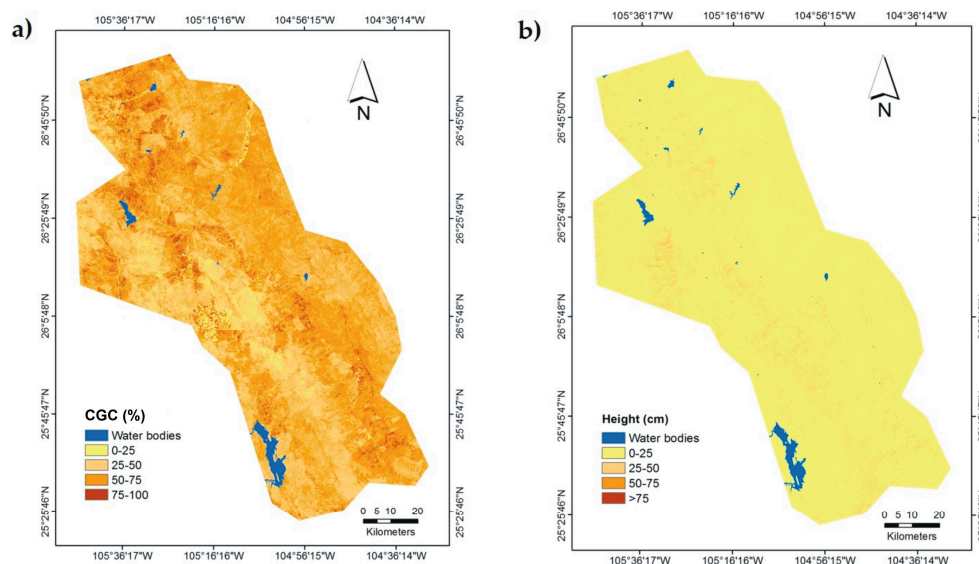

Figure 4. (**a**) Coverage of grass canopy (CGC) and (**b**) grass height distributions for 2009.
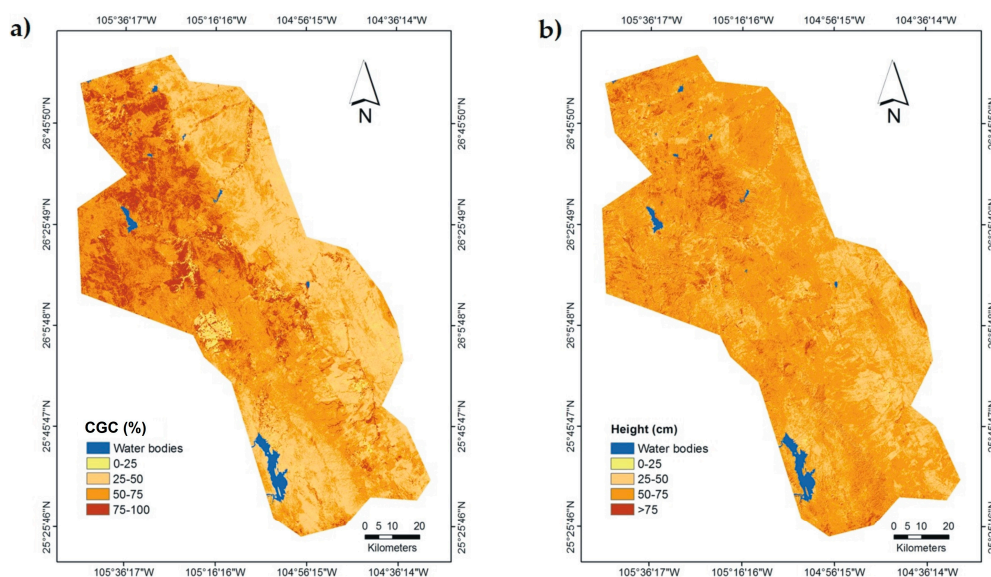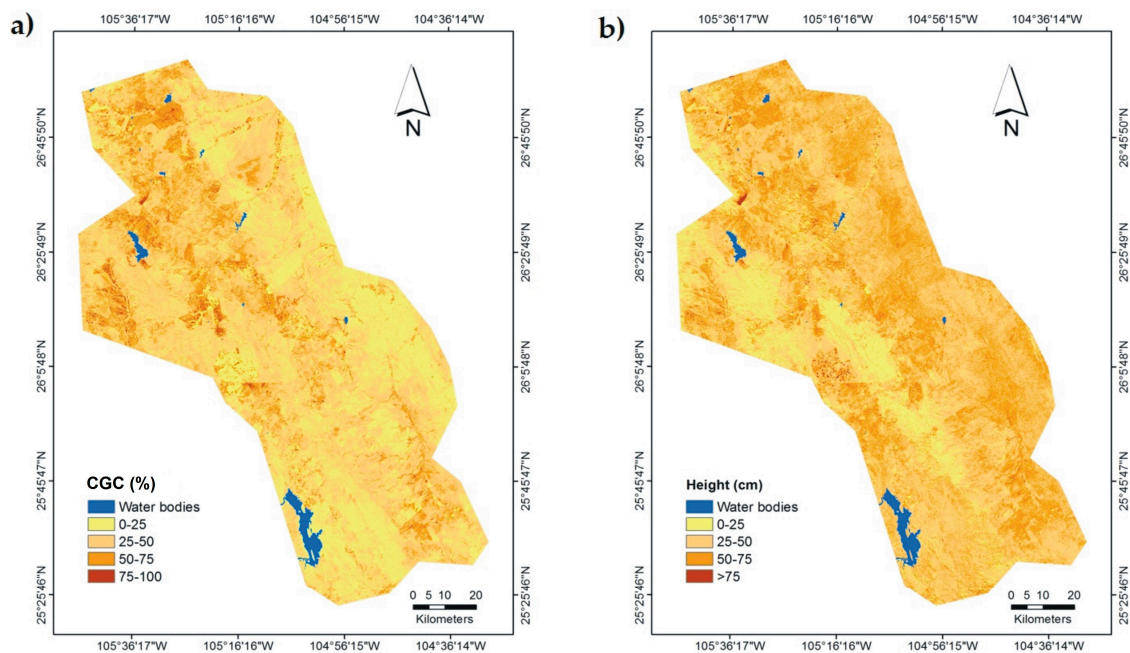

Figure 5. (**a**) Coverage of grass canopy (CGC) and (**b**) grass height distributions for 2010.

Figure 6. (**a**) Coverage of grass canopy (CGC) and (**b**) grass height distributions for 2011.

According to the Kappa index, the CGC images exhibit a moderate agreement among them. In the case of the variable grass height, the highest agreement occurred between 2010 and 2011 (Table 5). In the case of the variable CGC, the greatest agreement was observed the years 2009 and 2010. The lowest agreement between the images was obtained for the variable grass height when comparing 2009 and 2010, as well as 2009 and 2011, which can be explained by the large surface area with a low grass height showed in the map of 2009. The field data showed lower mean and statistical differences for this year, as mentioned above. However, the best agreement between maps of 2010 and 2011 does not necessarily mean a spatial correspondence between the variables. Thus, an area with high CGC does not necessarily correspond to an area with a high grass height of the grassland. Moreover, although the descriptions of the variable distribution were generally completed, various degrees of structural heterogeneity can be appreciated with a greater detail in the maps.

Table 5. Kappa index between the maps for Coverage of Grass Canopy (CGC) and grass height during the three years studied.

CGC			
2009	**2010**	**2011**	
1	0.59 **	0.56 **	2009
	1	0.49 **	2010
Grass Height			
2009	**2010**	**2011**	
1	0.36 *	0.40 *	2009
	1	0.59 **	2010

* weak and ** moderate agreements.
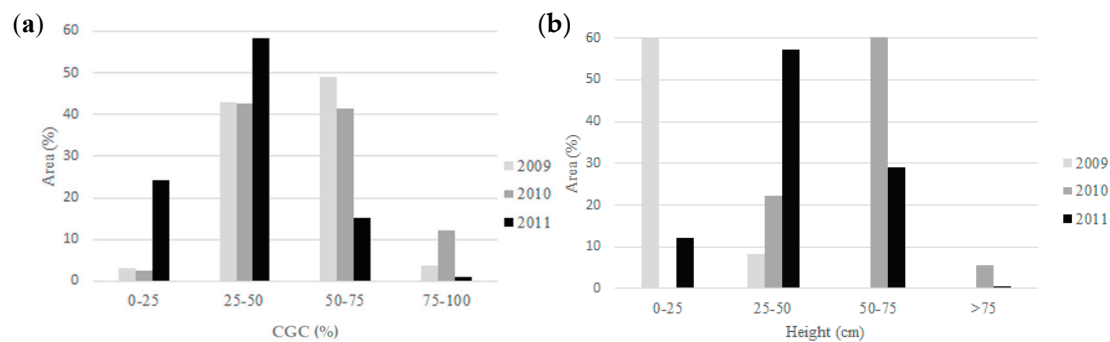
Figure 7. Area in percentages occupied by the ranges of (**a**) Coverage of Grass Canopy (CGC) and (**b**) grass height in the region Cuchillas de la Zarca.

4. Discussion

In the literature, there is a diversity of papers similar to this study in which the coefficients of determination are lower or similar, especially in cases where the same sensor is used [23,25]. The precision of the results may be partially due to the method of obtaining information in the field, the characteristics of the sensor (i.e., temporal and spatial resolution) and its age, the type of ecosystem, as well as the statistical analyses carried out. The latter appears to substantially affect the fit of the models between the data from the field and the sensor data [40–43]. Although some studies have obtained a good fit with the use of a limited number of bands [25,42], others studies [23] have required the interaction of a greater number of bands, indices or synthetic bands to achieve a better fit, as it was the case in this study. It is worth mentioning that the models selected for one year may not be appropriate to be used for a different year, because the images from different years have different digital values [44]. Possibly, a good fit on the models was not achieved with the data from the images due to an unsatisfactory correction of the data, which did not allow the use of a single model for each variable for the three years [45].

To explain the slight quantitative differences between the CGC maps, the study of Khumalo and Holechek [46] was considered. They found that the precipitation of the previous year is one of the major factors that are associated with biomass production in grasslands of the Chihuahuan Desert in southern New Mexico. Their results showed that individually, precipitation in August is the variable most highly correlated to the grassland condition. When analyzing the drought data for the three years, the presence of this phenomenon was not observed in the area during this month [38]. This may explain why there were basically no differences in the Kappa index of CGC for the three years. Therefore, for these variations among the years, other aspects such as spatial variation in grazing, forest fires and the phenology of the grass species should be considered. The CGC levels recorded during the three winter seasons studied could have enabled different species of wildlife, such as migratory grassland birds, to find this important habitat requirement [47].

The high reflectance values for the middle-infrared and near-infrared bands correspond to the general pattern of spectral behavior in vegetated surfaces [42]. The highest values for bands 2–4, 7 in 2011 may indicate high moisture contents in the soil as well as vegetation vigor. The latter factor may be attributed to the photosynthetic activity of perennial grasses, which grow and develop during the rains of February. However, according to the comparison of the maps, this difference does not seem to have greater repercussions with respect to the marked differences between the levels of CGC and grass height between 2010 and 2011. The decline in reflectance values of the bands 1–3 in some of the quadrants in the central and the southeastern zones, seems to be more associated with the particular characteristics of the composition and structure of the vegetation in some transects, since the resulting maps did not reflect the same pattern.

The CGC and grass height showed quantitative inter-annual fluctuations and spatio-temporal variations without an apparent specific pattern. Jin et al. [48] found similar results for biomass, which is

directly related to CGC and grass height. The greatest quantitative variation was registered for the variable height, which was possibly due to the fact that this variable is more susceptible to changes than CGC. This may be related to the grasses' characteristics, such as senescence [49]. In addition, when grazing is practiced in an area, the height of the grassland is the first variable affected. However, and similar to the variable CGC, other abiotic factors should be discarded, such as climate variables, which may affect the characteristics of the grassland [50,51].

The spatial heterogeneity observed in all the maps on a larger scale, agreed with the results found in other studies [48,52]. Even though in our study we found evidence of spatial gradients, these were not as marked as the ones found at the larger scale. Among other things, this element allows the presence of various species of grassland birds that have different CGC and grass height requirements during the winter season [14]. Hence, it has been found that the CUZA region is an area of high diversity of not only bird species, but also of some others, such as grasses and forbs [53,54]. According to McGranahan et al. [55], additional factors that could influence this heterogeneity are fires and grazing.

The maps generated for CGC and grass height showed moderately high accuracies that can be representative and used as a reference to help assess current and future land use development, grasslands capacities, animal production potentials and the status of grassland avian habitats [41,56–58].

5. Conclusions

Through the use of images of the Landsat TM5 sensor, it was possible to predict the spatial distribution of CGC and grass height of a grassland, using linear models in combination with field data. Although a field validation was not performed, the maps contributed to the understanding of the characteristics and dynamics of the Chihuahuan Desert grasslands. The information generated may serve to establish better strategies for monitoring grasslands and determine those areas that are most relevant for conservation. In addition, the methodology implemented in this study can be applied to perform a program for monitoring the grassland condition.

A benefit of the methodology applied in this study is the ability to identify and focus fragmented and degraded areas. Other benefits include the capacity to extrapolate from limited ground monitoring locations with increased confidence to the possibility of monitoring inaccessible areas, as well as to analyze changes across the landscape over time.

The maps obtained with this approach can be used as layers to model the potential distribution of migratory grassland birds given that the structural characteristics of vegetation are among the main factors that determine their distribution in the area.

Author Contributions: José Hugo Martínez-Guerrero, Alfredo Pinedo-Alvarez and Alberto Rodríguez-Maturino conceived and designed the methodology. Alberto Rodríguez-Maturino performed the field sampling and produced the first draft. Emilio Pereda-Solis and Isaías Chairez-Hernández analyzed the data. Federico Villarreal-Guerrero and Marusia Rentería-Villalobos substantially contributed to the discussions, revisions and editions of the manuscript.

Conflicts of Interest: The authors declare no conflict of interest.

References

1. Adams, J.M.; Hugues, F.; Denard, F.L.; McGlade, J.; Woodward, I.F. Increases in Terrestrial Carbon Storage from the Last Glacial Maximum to the Present. *Nature* **1990**, *348*, 711–714. [CrossRef]
2. Peng, J.; Zhenhuan, L.; Yinghui, L.; Jiansheng, W.; Yinan, H. Trend Analysis of Vegetation Dynamics in Qinghai. Tibet Plateau using Hurst Exponent. *Ecol. Indic.* **2012**, *14*, 28–39. [CrossRef]
3. Herrera, A.Y.; Cortes, O.A. Listado Florístico y Aspectos Ecológicos de la Familia Poaceae Para Chihuahua, Durango y Zacatecas, México. *J. Bot. Res. Inst. Tex.* **2010**, *4*, 711–738.

4. Pool, D.B.; Panjabi, A.O.; Macias, D.; Solhjem, M. Rapid Expansion of Croplands in Chihuahua, Mexico Threatens Declining North American Grassland Bird Species. *Biol. Conserv.* **2014**, *170*, 274–281. [CrossRef]

5. Manjarrez, D.C.; Pinedo, A.A.; Pinedo, A.C.; Villarreal, G.F.; Cortes, P.L. Vegetation Landscape Analysis due to Land Use Changes on Arid Lands. *Pol. J. Ecol.* **2015**, *63*, 272–279. [CrossRef]

6. Hoekstra, M.J.; Boucher, T.M.; Taylor, H.R.; Carter, R. Confronting a Biome Crisis: Global Disparities of Habitat Loss and Protection. *Ecol. Lett.* **2005**, *8*, 23–29. [CrossRef]

7. USGS (United States Geological Survey). The North American Breeding Bird Survey, Results and Analysis 1966–2012. Available online: http://www.mbr-pwrc.usgs.gov/bbs/ (accessed on 5 May 2014).

8. Macias, D.A.; Montoya, A.B.; Gonzalez, M.C.E.; Rodriguez, S.J.R.; Hunt, W.G.; Krannitz, P.G. Factors Influencing Habitat Use by Migratory Grassland Birds in the State of Chihuahua, Mexico. *Auk* **2009**, *126*, 896–905. [CrossRef]

9. Guo, Q.; Zhongmin, H.; Shenggong, Li.; Xuanran, L.; Xiaomin, S.; Guirui, Y. Spatial Variations in Aboveground Net Primary Productivity Along a Climate Gradient in Eurasian Temperate Grassland: Effects of Mean Annual Precipitation and Its Seasonal Distribution. *Glob. Chang. Biol.* **2012**, *18*, 3624–3638. [CrossRef]

10. Reichmann, G.L.; Sala, E.O.; Debra, P.C. Precipitation Legacies in Desert Grassland Primary Production Occur through Previous-Year Tiller Density. *Ecology* **2013**, *94*, 435–443. [CrossRef] [PubMed]

11. Granados, S.D.; Sanchez, G.A.; Granados, R.L.V.; De la Rosa, B.A. Ecología de la Vegetación del Desierto Chihuahuense. *Revista Chapingo. Serie Ciencias Forestales y del Ambiente* **2011**, *17*, 111–130. [CrossRef]

12. Arellano, E.C.; Vidal, L.J.C.; García, H.L.; Laundré, W.J.; Reza, C.F.; Mejia, M.F.M.; Vargas, R.M.; Galaviz, D.L.F.; Romero, G.A.; Spilsbury, M.A. Registro de Presencia y Actividades de Algunos Mamíferos en el Desierto Chihuahuense, México. *THERYA* **2014**, *5*, 793–816. [CrossRef]

13. Manzano, P.; List, R. Grasslands of Mexico: A Perspective on Their Conservation. In Proceedings of the Grasslands Ecosystems, Endangered Species, and Sustainable Ranching in the Mexico-U.S. Borderlands, Conference Proceedings, Fort Collins, CO, USA, 2006; Basurto, X., Hadley, D., Eds.; United States Department of Agriculture: Erie, KS, USA, 2006; pp. 43–47.

14. Martínez, G.J.H.; Pereda, S.M.E.; Wehenkel, C. Association of Ammodramus Bairdii A. 1844, and Other Species of grassland Granivorous Birds in Winter Time in Northwestern Mexico. *Open J. Ecol.* **2014**, *4*, 281–288. [CrossRef]

15. Czerwinski, C.J.; Douglas, J.K.; Scott, W.M. Mapping Forest Growth and Decline in a Temperate Mixed Forest Using Temporal Trend Analysis of Landsat Imagery, 1987–2010. *Remote Sens. Environ.* **2014**, *141*, 188–200. [CrossRef]

16. Vittek, M.; Brink, A.; Donnay, F.; Simonetti, D.; Desclée, B. Land Cover Change Monitoring Using Landsat MSS/TM Satellite Image Data over West Africa between 1975 and 1990. *Remote Sens.* **2014**, *6*, 658–676. [CrossRef]

17. Goward, S. N.; Masek, G.J.; Williams, L.D.; Irons, R.J.; Thompson, R.J. The Landsat 7 Mission: Terrestrial Research and Applications for the 21st Century. *Remote Sens. Environ.* **2001**, *78*, 3–12. [CrossRef]

18. Wulder, A.M.; Masek, G.J.; Cohen, B.W.; Loveland, R.T.; Woodcock, E.C. Opening the Archive: How Free Data Has Enabled the Science and Monitoring Promise of Landsat. *Remote Sens. Environ.* **2012**, *122*, 2–10. [CrossRef]

19. Hansen, M.C.; Loveland, T.R. A Review of Large are Monitoring of Land Cover Change Using Landsat data. *Remote Sens. Environ.* **2012**, *122*, 66–74. [CrossRef]

20. Coppin, P.; Jonckheere, I.; Nackaerts, K.; Muys, B.; Lambin, E. Digital Change Detection Methods in Ecosystem Monitoring: A Review. *Int. J. Remote Sens.* **2004**, *25*, 1565–1596. [CrossRef]

21. Krofcheck, D.J.; Eitel, U.H.J.; Vierling, A.L.; Schulthess, U.; Hilton, M.T.; Dettweiler, R.E.; Pendleton, R.; Litvak, E.M. Detecting Mortality Induced Structural and Functional Changes in a Piñon-Juniper Woodland Using Landsat and RapidEye Time Series. *Remote Sens. Environ.* **2014**, *151*, 102–113. [CrossRef]

22. Schmitt, H.M.; Sweeney, P.S.; Evans, P.T. Classification of Coffee-Forest Landscapes Using Landsat TM Imagery and Spectral Mixture Analysis. *Photogramm. Eng. Remote Sens.* **2013**, *79*, 457–468. [CrossRef]

23. Sivanpillai, R.; Ewers, E.B. Relationship between Sagebrush Species and Structural Characteristics and Landsat Thematic Mapper data. *Appl. Veg. Sci.* **2013**, *16*, 122–130. [CrossRef]

24. Pucheta, E.E.; Heil, F.L.; Schneider, C. Modelos de Regresión Para la Estimación de la Biomasa Aérea en un Pastizal de Montaña de Pampa de Achala. (Córdoba, Argentina). *AGRISCIENTIA* **2004**, *21*, 23–30.

25. Manrique, S.; Nuñez, V.; Franco, J.; Seghezzo, L. Prediccion de Biomasa Natural a Partir de Sensores Remotos en el Valle de Lerma. *Avances en Energías Renovables y Medio Ambiente* **2010**, *14*, 63–70.

26. Calvert, M.A.; Walde, J.S.; Taylor, D.P. Non-breeding Drivers of Population Dynamics in Seasonal Migrants: Conservation Parallels Across Taxa. *Avian Conserv. Ecol.* **2009**, *4*, 5. [CrossRef]

27. Chaneton, J.E. Factores que Determinan la Heterogeneidad de la Comunidad Vegetal en Diferentes Escalas Espaciales. In *La Heterogeneidad de la Vegetación de los Agroecosistemas*; Oesterheld, M., Aguiar, M.R., Ghersa, C.M., Paruelo, J.M., Eds.; Editorial Facultad de Agronomía-UBA: Buenos Aires, Argentina, 2005; pp. 19–42.

28. Hoyt, A.C. The Chihuahuan Desert: Diversity at Risk. *Endanger. Species Bull.* **2002**, *27*, 16–17.

29. Rzedowski, J. *Vegetación de México*; Limusa: Mexico City, México, 1981; p. 504.

30. De León, M.D.; Pinedo, A.A.; Martínez, G.J.H. Aplicación de Sensores Remotos en el Análisis de la Fragmentación del Paisaje en Cuchillas de la Zarca, México. *Investigaciones Geográficas, Boletín del Instituto de Geografía* **2014**, *84*, 42–53. [CrossRef]

31. CONABIO. (Comisión Nacional para el Conocimiento y Uso de la Biodiversidad). Catálogo de Metadatos Geográficos. Red de Carreteras Escala 1:10,000,000. Available online: http://www.conabio.gob.mx/informacion/metadata/gis/carre1mgw.xml?_xsl=/db/metadata/xsl/fgdc_html.xsl&_indent=no (accessed on 16 October 2017).

32. Crist, P.E.; Richard, C.C. A Physically Based Transformation of Thematic Mapper Data-The TM Tasseled Cap. *IEEE Trans. Geosci. Remote Sens.* **1984**, *22*, 256–263. [CrossRef]

33. Chander, G.; Markham, L.B.; Helder, L.D. Summary of Current Radiometric Calibration Coefficients for Landsat MSS, TM, ETM+, and EO-1 ALI Sensors. *Remote Sens. Environ.* **2009**, *113*, 893–903. [CrossRef]

34. Chuvieco, S.E. *Teledetección Ambiental: La Observación de la Tierra Desde el Espacio*; Ariel Ciencia: Barcelona, Spain, 2002.

35. Dobson, J.A.; Barnett, A. *An Introduction to Generalized Linear Models*; Taylor & Francis Group: New York, NY, USA, 2008.

36. Rosenfield, H.G.; Fitzpatric, K.L. A Coefficient of Agreement as a Measure of Thematic Classification Accuracy. *Photogramm. Eng. Remote Sens.* **1986**, *52*, 223–227.

37. Eastman, R.J. *Idrisi Selva*; Version 17; Clark Labs, Clark University: Worcester MA, USA, 2012.

38. SMN. Monitor de Sequía de México. Available online: http://smn.cna.gob.mx (accessed on 15 January 2014).

39. Wiles, L.J.; Dunn, G.; Printz, J.; Patton, B.; Nyren, A. Spring Precipitation as a Predictor for Peak Standing Crop of Mixed-Grass Prairie. *Rangel. Ecol. Manag.* **2011**, *64*, 215–222. [CrossRef]

40. Cohen, B.W.; Maiersperger, K.T.; Gowerc, T.S.; Turner, P.D. An Improved Strategy for Regression of Biophysical Variables and Landsat ETM+ Data. *Remote Sens. Environ.* **2003**, *84*, 561–571. [CrossRef]

41. Xie, Y.; Sha, Z.; Yu, M.; Bai, Y.; Zhang, L. A Comparison of Two Models with Landsat Data for Estimating above Ground Grassland Biomass in Inner Mongolia, China. *Ecol. Model.* **2009**, *220*, 1810–1818. [CrossRef]

42. Gasparri, I.; Parmuchi, M.G.; Bono, J.; Karszenbaum, H.; Montenegro, C.L. Assessing Multi-Temporal Landsat ETM+ Images for Estimating Above-Ground Biomass in Subtropical Dry Forests of Argentina. *J. Arid Environ.* **2010**, *74*, 1262–1270. [CrossRef]

43. Karl, W.J. Spatial Predictions of cover Attributes of Rangeland Ecosystems Using Regression Kriging and Remote Sensing. *Rangel. Ecol. Manag.* **2010**, *63*, 335–349. [CrossRef]

44. Song, C.; Woodcock, E.; Seto, C.K.; Lenney, P.M.; Macomber, A.S. Classification and Change Detection Using Landsat TM data: When and How to Correct Atmospheric Effects? *Remote Sens. Environ.* **2001**, *75*, 230–244. [CrossRef]

45. Lencinas, D.J.; Bell, M.D. Estimación de Clases de Edad de las Plantaciones de la Provincia de Corrientes, Argentina, con Base en Datos Satelitales Landsat. *Bosque* **2007**, *28*, 106–118. [CrossRef]

46. Khumalo, G.; Holechek, J. Relationships between Chihuahuan Desert Perennial Grass Production and Precipitation. *Rangel. Ecol. Manag.* **2005**, *58*, 239–246. [CrossRef]

47. Yahner, H.R. *Wildlife Behavior and Conservation*; Springer Science: New York, NY, USA, 2012.

48. Jin, Y.; Yang, X.; Qiu, J.; Li, J.; Gao, T.; Wu, Q.; Zhao, F.; Ma, H.; Yu, H.; Xu, B. Remote Sensing-Based Biomass Estimation and Its Spatio-Temporal Variations in Temperate Grassland, Northern China. *Remote Sens.* **2014**, *6*, 1496–1513. [CrossRef]

49. Duru, M.; Ducrocq, H. Growth and Senescence of the Successive Grass Leaves on a Tiller. Ontogenic Development and Effect of Temperature. *Ann. Bot.* **2000**, *85*, 635–643. [CrossRef]

50. Westoby, M.; Walker, B.; Noy-Meir, I. Opportunistic Management for Rangelands Not at Equilibrium. *J. Range Manag.* **1989**, *42*, 266–274. [CrossRef]

51. Si, Y.; Schlerf, M.; Zurita, M.R.; Skidmore, A.; Wang, T. Mapping Spatio-Temporal Variation of Grassland Quantity and Quality Using MERIS Data and the PROSAIL Model. *Remote Sens. Environ.* **2012**, *121*, 415–425. [CrossRef]

52. Gao, T.; Yang, X.; Jin, Y.; Ma, H.; Li, J.; Yu, H.; Yu, Q.; Zheng, X.; Xu, B. Spatio-Temporal Variation in Vegetation Biomass and Its Relationships with Climate Factors in the Xilingol Grasslands, Northern China. *PLoS ONE* **2013**, *8*, e83824. [CrossRef] [PubMed]

53. Martínez, G.J.H.; Wehenkel, C.; Pereda, S.E.; Panjabi, A.; Levandoski, G.; Corral, R.J.; Díaz, M.R. Relación Entre la Cobertura del Suelo y Atributos de la Vegetación Invernal con *Ammodramus Bairdii*, Audubon 1844, en el Noroeste de México. *Agrociencia* **2011**, *45*, 443–451.

54. Hovick, J.T.; Elmore, D.R.; Fuhlendorf, D.S. Structural Heterogeneity Increases Diversity of Non-Breeding Grassland Birds. *Ecosphere* **2014**, *5*, 1–13. [CrossRef]

55. McGranahan, A.D.; Raicovich, M.G.; Wilson, N.W.; Smith, K.C. Preliminary Evidence that Patch Burn-Grazing Creates Spatially Heterogeneous Habitat Structure in Old-Field Grassland. *Southeast. Nat.* **2013**, *12*, 655–660. [CrossRef]

56. Moreau, S.; Bosseno, R.; Gu, X.; Baret, F. Assessing the Biomass Dynamics of Andean Bofedal and Totora high-Protein Wetland Grasses from NOAA/AVHRR. *Remote Sens. Environ.* **2003**, *85*, 516–529. [CrossRef]

57. Martin, L.M.; Moloney, K.A.; Wilsey, B.J. An Assessment of Grassland Restoration Success Using Species Diversity Components. *J. Appl. Ecol.* **2005**, *42*, 327–336. [CrossRef]

58. Kawamura, K.; Akiyama, T.; Yokot, H.; Tsutsumi, M.; Yasuda, T.; Watanabe, O.; Wang, S. Quantifying Grazing Intensities Using Geographic Information Systems and Satellite Remote Sensing in the Xilingol Steppe Region, Inner Mongolia, China. *Agric. Ecosyst. Environ.* **2005**, *107*, 83–93. [CrossRef]